

Cosmic Dawn Intensity Mapper: Spacecraft and Mission Design for a Probe-Class Space Telescope

Philip Linden^{1,†}, Michael Zemcov²

¹*Department of Mechanical Engineering, Kate Gleason College of Engineering, Rochester Institute of Technology, Rochester, NY 14623, USA, pjl7651@rit.edu*

²*Center for Detectors, School of Physics and Astronomy, Rochester Institute of Technology, Rochester, NY 14623, USA, zemcov@cf.d.rit.edu*

Received (to be inserted by publisher); Revised (to be inserted by publisher); Accepted (to be inserted by publisher);

Cosmic Dawn Intensity Mapper (CDIM) is a Probe-class near-IR space telescope with the scientific goal of conducting large spectro-imaging surveys over a five-year period in the 2020 Decadal. A high-level system architecture was designed to identify key features and technologies aboard the CDIM spacecraft in preparation for more detailed studies such as a Team-X session at NASA Jet Propulsion Laboratory.

Keywords: spacecraft, telescope, system, cryogenic, infrared, design.

1. Introduction

Observing the behavior and characteristics of the earliest stars and galaxies is fundamental to understanding the physics that led to their formation and evolution. Breakthrough discoveries in understanding the physics of the epoch of reionization are anticipated in the 2020–2030 decade thanks to the Wide Field Infrared Survey Telescope (WFIRST) and James Webb Space Telescope (JWST). However, JWST’s capability will be limited to **only several** cosmological deep fields. Although WFIRST will be capable of wide area surveys, its spectroscopy is limited to $2\mu\text{m}$ and thus limits the selection of galaxies it is able to observe. Neither JWST nor WFIRST provide a complete understanding of the epoch of reionization, specifically in terms of answering the questions of when and how the universe came to be. This area of research is a prime candidate for a Probe class mission optimized to study reionization.

Probe class missions occupy a role on a larger scale than Discovery missions, such as Kepler and Dawn, but not as vast as Flagship missions such as JWST (Wiseman *et al.*, 2015). Such missions are intended to be PI-led scientific investigations rather than general observatories, and have a firm \$1B cap.

Cosmic Dawn Intensity Mapper (CDIM) is a concept for a Probe class 1.5m aperture telescope, passively cooled to 45 K, with a 6×6 detector array that utilizes linear variable filters (LVFs) and actively cooled to 35 K (Cooray *et al.*, 2016), capable of three-dimensional spectro-imaging observations over the wavelength range of 0.75 to $7.5\mu\text{m}$, at a spectral resolving power $\Delta\lambda/\lambda$ of 500. CDIM has a 10deg^2 instantaneous field of view (FoV) utilizing linear variable filters (LVFs) atop a focal plane of thirty-six 2048×2048 detectors. The survey strategy using spacecraft operations following a shift and stare mode will result in 1360 independent narrow-band spectral images of the sky on a given location. Surveys could span from 25deg^2 up to 1000deg^2 over a five year lifetime in an orbit about Sun-Earth Lagrange point L_2 .

With these instrument requirements, CDIM is optimized to search for the first cosmic sources of dust and evidence of the very earliest stellar populations, bridging the gaps in the JWST and WFIRST cosmic dawn surveys and exceeding them in capability.

[†]Corresponding author.

Table 1. Critical design requirements for the CDIM spacecraft following the format suggested by Wertz *et al.*

Spacecraft Design Driver	Impact	Target
Cost	Quality of parts	less than \$1 B
Mass	Launch vehicle	less than 1000 kg
Temperature (OTA)	Cryocooler, radiator	45 K
Temperature (Detector)	Cryocooler, radiator	35 K
Pointing Requirements	Attitude control sys	less than 0.5 arcsec
Lifetime	Redundancy, RCS propellant	5 years
Orbit	Solar array, thermal management, launch vehicle, telemetry	Sun-Earth L ₂

2. Optical Telescope Assembly

Preliminary explorations indicate that a 1.5 m aperture off-axis primary mirror cooled to 45 K is required to meet CDIM’s spectro-imaging requirements (Cooray *et al.*, 2016). The primary mirror is notionally assumed to be constructed from light-weighted Corning (ultra-low expansion) silica-titania glass with a honeycomb core and a gold-deposition surface coating. “Back-of-the-envelope” calculations estimate the primary mirror’s mass to be roughly 200 kg.

Multiple detectors satisfy CDIM’s spatial resolution, wavelength range, and sensitivity requirements. These detectors range in TRL, but all are sufficiently developed to be considered for the 2020 Decadal and will be demonstrated on missions such as NEOCam, SPHEREx, and JWST.

Teledyne H2RG-18 HyViSI detectors offer a 2048×2048 pixel array format at a pixel pitch of $18 \mu\text{m}$ (Bai *et al.*, 2008). CDIM will utilize a 6×6 H2RG array. Each detector nominally dissipates less than 4 mW, for a total power dissipation of less than 150 mW for the array.

CDIM optics, instruments, and focal plane will be housed in a light-tight box. The optical telescope assembly (OTA) as a whole is estimated to have a mass of x kg.

3. Thermal Regulation

CDIM employs both passive and active thermal regulation systems. By using passive radiators in tandem with an active cryocooler, the static OTA heat load can be dissipated by the lightweight radiator and a smaller cryocooler may be used to only cool the detector array rather than the whole OTA mass plus focal plane assembly.

The OTA is cooled to 45 K passively to reduce background photon load in the near-IR. Passive thermal regulation is maintained using a V-groove radiator, which bounces radiative heat into the 3 K background of space. V-groove radiators have been demonstrated in passive cryogenic radiators up to 4 K with Planck, SPIRIT, and Spitzer (warm mission). In order to achieve passive cooling from a baseline temperature of 300 K at Sun-Earth Lagrange point L₂, a x -stage V-groove radiator with an area of $x \text{ m}^2$ is required.

The CDIM detector array is actively cooled to 35 K to reduce thermal noise. Stirling-cycle mechanical refrigerators are low-vibration, high-reliability, and lightweight active cryocooling systems that have significant heritage in space applications. One candidate system is Raytheon’s PSC 1-stage Stirling cryocooler, capable of cooling a 1.2 W parasitic heat load to 35 K. This cryocooler is 18.6 kg and requires 88 W of input power (Donabedian *et al.*, 2003).

4. Attitude Determination and Control

To conduct a survey, the spacecraft must first understand its orientation and then act to align itself with a given area of the sky. Redundant systems of varying levels of fidelity are included to allow CDIM to operate in different power states. Low-fidelity attitude determination sensors such as sun sensors are cheap, accurate to less than one degree, and lightweight.

High-fidelity attitude determination is conducted by star tracking cameras. Star trackers identify constellations in their field of view to determine the spacecraft’s heading to within 1 arcsecond.

In a heliocentric orbit, the primary disturbance to the spacecraft’s heading is solar radiation pressure (SRP). At L₂, solar radiation pressure presents itself as a constant torque on the spacecraft on the order of

10^{-5}N m .

Cold-gas or hydrazine thrusters will be used for orbit station-keeping as well as momentum management. A desired heading is maintained by the spacecraft using a 3-axis zero-momentum inertial system, whereby the error in heading due to SRP is cancelled out by spinning up or slowing down reaction wheels. Reaction wheel systems are capable of torques ranging from .01 to 1N m and store 0.4 to 3000N m s of practical momentum (Wertz *et al.*, 2015). Power consumption varies with reaction wheel speed, with a maximum estimate of roughly 100 W. Since SRP is constant, after some time the inertial attitude control will become saturated. Desaturation is managed by engaging station-keeping thrusters for short periods of time.

5. Flight Computer

CDIM is capable of autonomous operation and system diagnostics. Nominal operation includes maintaining a heading during imaging, capturing images, and downlinking data to Earth. Images will be processed as demonstrated by the Spectro Photometer for the History of the Universe, Epoch of Reionization, and Ices Explorer (SPHEREx).

6. Telemetry

Typically for high-Earth and deep-space missions, the X-Band Space Science frequency band is used for uplink and downlink between the spacecraft and Ground Stations. Thus, high-gain antennas are best suited for both links (Wertz *et al.*, 2015).

A survey conducted by CDIM will generate 168.39 Gb of data per day employing on-board data processing akin to SPHEREx. With a compression ratio of 2.5:1, CDIM will downlink a total of 63.7 Gb/day during a survey. Transmission rates are dependent on the total time available for CDIM to send data to a ground station. For example, the spacecraft could transmit continuously at a very low transfer rate, or send larger volumes of data once per day over 1 hour at the expense of a higher transfer rate.

Uplinks will follow standard protocols and not require transmitting large volumes or particularly fast transfer rates.

Table 2. For redundancy, CDIM is outfitted with multiple communication modes. Downlink transfer rates reflect estimates based on the target of 63.7 Gb/day. Typical data transfer rates are outlined for uplinks (Wertz *et al.*, 2015).

Mode	Uplink	Downlink
Emergency	7.8 bps	5–10bps
Engineering data	15.6–2000kbps	Up to 10 bps
Science data	15.6–2000kbps	0.74 Mbps (continuous) or 17.7 Mbps (1 hour per day)

7. Power

All power generation will come from an array of photovoltaic cells facing the sun. In order to survey the entire sky, the cells must be able to adjust to account for different incident angles to the sun. The array must deploy after the launch and orbital insertion phases of the mission.

Based on a rough power budget and the spacecraft's position at L2, the array must be $x\text{m}^2$ in area to sustain operation. The dark side of the array acts as a radiator to contribute to the thermal regulation of the spacecraft bus.

8. Structure

The spacecraft bus houses all non-instrumentation systems including the cryocooler, ADCS, and power modules. It would have approximately some dimensions and be made of standard materials. The bus will

Table 3. Available launch vehicle configurations and their capabilities to send payloads to L₂ (Rioux, 2016; Space Launch Report).

Vehicle	Payload to L ₂	Fairing size	Cost
Falcon 9 v1.1	2900 kg	5.2×13.1 m	\$90M
Falcon Heavy*	14 000 kg	5.2×13.1 m	\$62M
Atlas V 551	6100 kg	4.2×10.0 m 5.1×11.0 m	\$153M
Ariane V	6600 kg	5.4×12.7 m	\$165M
		5.4×13.8 m	
		5.4×17.0 m	\$220M
Delta IV Heavy	9800 kg	5.0×14.3 m	\$375M
		5.0×19.1 m	

* Costs and specifications are representative of launch vehicles that are currently available or in development.

also include hard points for integration with the launch vehicle.

9. Mission Profile

9.1. Launch Vehicle

CDIM is comfortably within the mass and spatial limits of currently available and development launch vehicles capable of delivering payloads to Sun-Earth Lagrange Point L₂.

9.2. Operations

9.3. End of Life

10. Cost Estimates

The overall cost of a space telescope may be broken down into a set of drivers whose influence is correlated with historical data. All conclusions based on statistical analysis are only as good as their databases. Fiscal data, such as what is required for proper analysis, is scarce. Estimations are made with engineering judgement based on available data. Multiple models are used to develop a reasonable cost model for CDIM.

To estimate the cost of the CDIM mission, estimations are separated into drivers of the *mission cost*, which includes hardware, development, ground support, integration, testing, science, and management. Existing generalized parametric cost estimation approaches identify key cost drivers for mission cost (Stahl *et al.*, 2013; Bely, 2011), but do not take labor or overhead costs into account. Overhead and labor costs are included in a more robust model for *total cost*, where:

$$\text{Total Cost} = \text{Mission Cost}(1 + \text{Factor}), \quad \text{Factor} = 0.5 \quad (1)$$

Stahl *et al.* present a statistical approach to estimating OTA cost based on correlations with data on flown space telescope missions. CDIM's projected costs may be obtained from these findings with engineering judgement, knowing that the data is drawn from a relatively small sample set.

The Stahl Model for OTA Diameter vs. OTA Cost in Figure 4 estimates a 1.5 m OTA mirror aperture diameter costing \$58.2M, which is comfortably within the OTA budget of \$62–85M from the Bely and Stahl Mission Cost Models in Table 1.

Choosing a 1.5 m telescope at \$58.2M as the driving factor on cost, alternative mission cost and total cost estimates may be derived from Stahl and Bely models as shown in Table 5. There is a significant

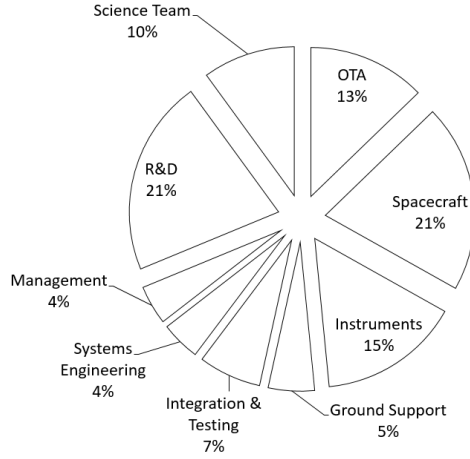


Fig. 1. CDIM estimated cost breakdown in percent of mission cost.

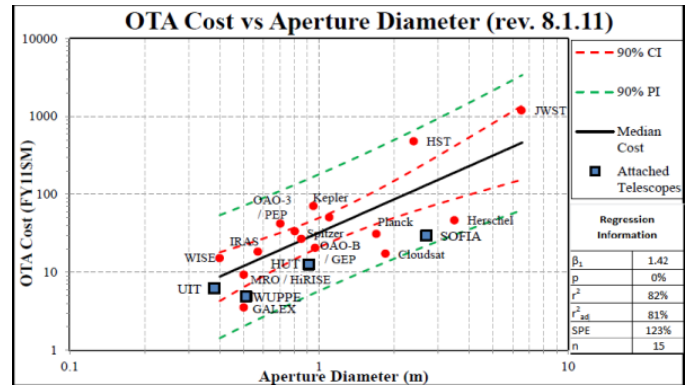


Fig. 2. Optical Telescope Assembly vs. cost correlation (Stahl *et al.*, 2013).

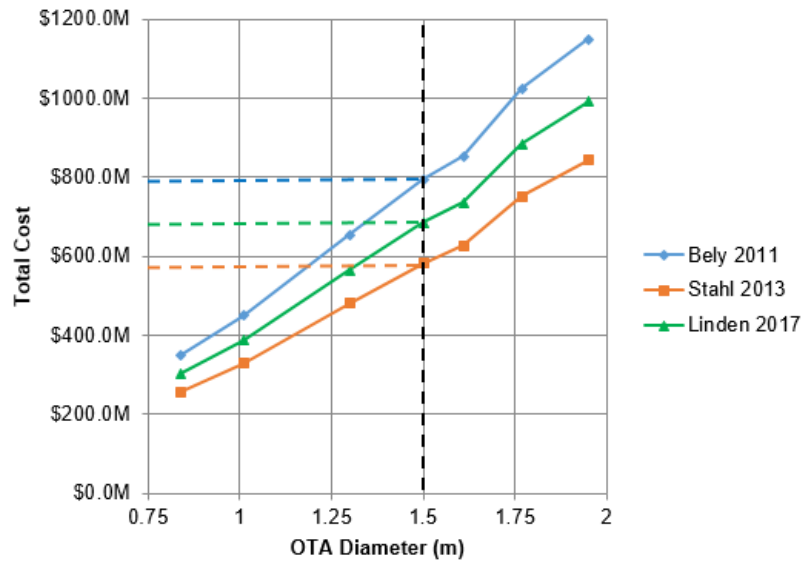


Fig. 3. CDIM total cost relation to OTA aperture diameter under various cost models. The model described here is robust and presents a conservative estimate compared to similar models by Bely and Stahl *et al.*, after a total cost approximation is applied following Equation 1.

(\$200M+) discrepancy between the Bely and Stahl cost models, but both estimations show that CDIM fits squarely within the range of a Probe class NASA mission. The Stahl OTA Diameter vs. OTA Cost model is based on a limited set of data and is not a perfect correlation, and does not account for influences that other parameters like operating temperature have on Mission Cost. It does show a reasonable correlation with historical data, however, and may be used for preliminary design phases for missions such as CDIM.

11. Conclusion

Acknowledgments

Thanks.

References

- Bai, Y., Bajaj, J., Beletic, J. W., Farris, M. C., Joshi, A., Lauxtermann, S., Petersen, A. & Williams, G. [2008] “Teledyne imaging sensors: silicon cmos imaging technologies for x-ray, uv, visible, and near infrared,” doi: 10.1117/12.792316, URL <http://dx.doi.org/10.1117/12.792316>.
- Bely, P.-Y. [2011] *The Design and Construction of Large Optical Telescopes* (Springer).
- Cooray, A., Bock, J., Burgarella, D., Chary, R., Chang, T.-C., Doré, O., Fazio, G., Ferrara, A., Gong, Y., Santos, M., Silva, M. & Zemcov, M. [2016] *ArXiv e-prints* .
- Donabedian, M., of Aeronautics, A. I., Astronautics & (Firm), K. [2003] *Spacecraft thermal control handbook* (Aerospace Press, El Segundo, Calif), ISBN 9781884989148.
- Rioux, N. [2016] “Getting to orbit: Launch vehicles,” .
- Space Launch Report [2017] “Launch vehicle datasheets,” <http://www.spacelaunchreport.com/>.
- Stahl, H. P., Henrichs, T., Luedtke, A. & West, M. [2013] *Optical Engineering* **52**, 091805, doi:10.1117/1.OE.52.9.091805, URL <http://dx.doi.org/10.1117/1.OE.52.9.091805>.
- Wertz, J. R., Everett, D. F. & Puschell, J. J. [2015] *Space mission engineering: the new SMAD* (Microcosm Press).
- Wiseman, J., Clampin, M., Danchi, W., Mather, J., Oegerle, W., Barry, R., Traub, W., Stapelfeldt, K., Lissauer, J., Borucki, W., Greene, T., Bennett, D. & Johnston, K. [2015] “Space-based “probe class” missions for exoplanet research,” https://science.gsfc.nasa.gov/667/whitepapers/ProbeClassMissions_whitepaper.pdf.